The published version is available at: http://dx.doi.org/10.1109/TMAG.2013.2242857

Iron Losses, Magnetoelasticity and Magnetostriction in Ferromagnetic Steel Laminations

Paavo Rasilo, Deepak Singh, Anouar Belahcen, Antero Arkkio

Aalto University School of Electrical Engineering, Department of Electrical Engineering, FI-00076, Aalto, Finland

The interdependence of iron losses and magnetoelasticity in ferromagnetic laminations is studied by numerical simulations. For the simulations, a finite-element model for the eddy currents in the lamination is coupled to a constitutive magnetomechanical material law. We demonstrate how the experimentally apparent rate-dependency of magnetostriction partly results from the comparison of the local surface magnetostriction to the average flux density supplied through the sheet. The average flux density is a global quantity and lags behind the local surface magnetostriction due to the skin effect of the eddy currents. Accurate modeling of the skin effect also shows that in addition to the hysteresis losses, the eddy-current losses also change as a result of applied mechanical stress, contrary to some earlier discussions in the literature.

***Index Terms*—Magnetic losses, magnetic materials, magnetomechanical effects, magnetostriction.**

I. Introduction

COUPLED magnetomechanical effects, or magnetoelasticity, in iron have been studied extensively both theoretically and experimentally [1]-[9]. The theoretical developments of Sablik and Jiles in [1] and [2] provide a physical background for the interdependency of the static magnetization properties and static magnetostriction, as well as their dependency on external mechanical loading. However, experimental observations have also shown dynamic hysteretic dependency of the magnetostriction on the supply flux density. The effect has been discussed by several authors up to recent years [4]-[7], but the attempts to model the phenomenon have so far been based on empirical models rather than describing its physical background [5], [7].

Another interesting experimental observation is the increase of iron losses due to applied mechanical stress [8], [9]. To discuss this effect, we briefly review Bertotti's statistical loss separation theory [10]. The theory considers a lamination with a thickness d and conductivity σ, through which a sinusoidally and unidirectionally varying average flux density with a frequency f and amplitude b_{av} is supplied. The total iron-loss power density p_{Fe} in the sheet is divided into hysteresis losses, macroscopic eddy-current losses, and microscopic excess eddy-current losses resulting from domain-wall motion, respectively:

$$p_{\mathrm{Fe}} = w_{\mathrm{hy}} f + \frac{\sigma d^2 \pi^2}{6} \left(f b_{\mathrm{av}} \right)^2 + c_{\mathrm{ex}} \left(f b_{\mathrm{av}} \right)^{1.5} . \qquad (1)$$

The hysteretic energy-loss density w_{hy} is rate independent, and thus the related power loss is directly proportional to the supply frequency. The classical eddy-current losses are analytically calculated by assuming a uniform flux-density distribution, i.e. constant value b_{av}, through the lamination thickness. The magnitude of the excess losses is defined by coefficient c_{ex}, which is experimentally determined from the difference between the measured total iron loss and the first two terms of (1). Due to this definition, underestimation in the hysteresis or macroscopic eddy-current losses would naturally result in overestimation of the excess losses. In [11], Mayergoyz concluded that accurate modeling of the skin effect typically results in larger classical eddy-current losses, and thus the excess losses are reduced by definition.

In [8], the authors concluded that only the hysteresis and excess losses are affected by mechanical loading, while the classical eddy-current losses stay unchangeable. Their analysis, however, was based on (1), the middle term of which neglects the skin effect and thus does not take into account the magnetization properties of the material. Similarly to the discussion in [11], it seems likely that at least part of the apparent increase in the excess losses can be explained by the change in the macroscopic eddy-current losses due to the changes in the magnetization properties with applied stresses.

In this paper we study if accurate skin-effect modeling can explain the aforementioned effects of dynamic magnetostriction and the increase in the iron losses due to applied stress without studying these phenomena at the domain-structure level. The approach is based on accurate modeling of the penetration of the magnetic field into the lamination with a unidirectional finite-element (FE) model coupled to a magnetomechanical material model. The results show that the skin effect indeed is a significant factor to consider when attempts are made to explain the physics behind the discussed phenomena.

II. Methods

A. Material Model

The scalar Sablik-Jiles-Atheron (SJA) model [1] is based on the assumption that a unidirectional stress τ is imposed parallel to the flux density b. The model is described by the following (differential) equations for the external field strength h, effective field strength h_{e}, total magnetization m, anhysteretic magnetization m_{a}, irreversible magnetization m_{i}, and magnetostriction λ:

$$h_{\mathrm{e}} = h + \alpha m + \frac{3}{2} \frac{\tau}{\mu_0} \frac{\partial \lambda \left(m_{\mathrm{a}} \right)}{\partial m_{\mathrm{a}}} , \qquad (2)$$

Manuscript received October 29, 2012. Corresponding author: P. Rasilo (e-mail: paavo.rasilo@aalto.fi).

$$m_{\mathrm{a}} = m_{\mathrm{s}}\left(\coth\frac{h_{\mathrm{e}}}{a} - \frac{a}{h_{\mathrm{e}}}\right), \tag{3}$$

$$\frac{dm_{\mathrm{i}}}{dh_{\mathrm{e}}} = \frac{m_{\mathrm{a}} - m_{\mathrm{i}}}{k\delta} \text{ with } \delta = \frac{dh/dt}{\left|dh/dt\right|}, \tag{4}$$

$$m = (1-c)m_{\mathrm{i}} + cm_{\mathrm{a}}, \tag{5}$$

$$b = \mu_0(h+m), \tag{6}$$

where μ_0 is the permeability of vacuum, and a, c, k, m_{s} and α are constant parameters. In [1] the magnetostriction was expressed as a function of the magnetization m as

$$\lambda(m) = -3\frac{\sqrt{1+r\phi(m_{\mathrm{s}})} - \sqrt{1+r\left(\phi(m_{\mathrm{s}}) - \phi(m)\right)}}{\sqrt{2Yr}}, \tag{7}$$

in which Y is the Young modulus, ν the Poisson ratio and we use the short-hand notation

$$r = \frac{9Y}{2b_{\mathrm{me}}^2(1+\nu)^2}, \tag{8}$$

in which b_{me} is the magnetoelastic coupling constant. The magnetic energy density is

$$\phi(m) = \frac{\mu_0}{2}\left(\alpha m^2 - 2\alpha'(m_{\mathrm{a}} - m)h + \alpha''(m_{\mathrm{a}} - m)^2\right), \tag{9}$$

in which parameters α' and α'' describe the hysteretic energy density.

The nine independent parameters of the model are the four parameters, a, c, k, and m_{s}, of the original Jiles-Atherton (JA) model, as well as Y, ν, b_{me}, α' and α''. In the SJA model, parameter α from the original JA model is dependent on the other mechanical and magnetoelastic parameters. In Section III, we first compare the dynamic magnetostriction results to measurements performed for a 0.5-mm Fe-Si sheet in the zero-stress case. Thus we apply the original JA model without the stress dependency and interpolate the magnetostriction from measured data instead of using (7). The model parameters are given in Table I.

In the study for the iron losses, the SJA model is applied with its parameters equal to those used in Fig. 1 of [1] and shown in Table I. However, the original works of Sablik and Jiles focused on very low-permeability steels and thus these parameters produce very flat b-h curves, the coercitivity fields of which are close to 2500 A/m. To make the b-h loop and thus the skin-effect model more realistic for Fe-Si sheets commonly used in electromagnetic devices, we scale the value of h output by the model by a factor 0.07. Although such scaling produces incorrect slope for the b-h loop at high saturation, the model still serves for the purpose of this paper before experimental stress-dependent magnetization data are available for comprehensive fitting of the model parameters.

Fig. 1 shows the hysteresis loops and the magnetostriction produced by the SJA model. The curves at stress values of -300, 0, and +300 MPa are shown, positive sign denoting tensile stress. The b-h curves meet at saturation when the magnetization approaches its saturation value m_{s}. The magnetostriction also has a hysteretic relationship to the field strength.

TABLE I
PARAMETERS OF THE MODEL

Parameter	Section III A	Section III B
α	$4.085 \cdot 10^{-4}$	-
a	156 A/m	4500 A/m
c	0.21	0.1
k	126 A/m	3000 A/m
m_{s}	$1.24 \cdot 10^{6}$ A/m	$1.61 \cdot 10^{6}$ A/m
Y	-	99.5 GPa
ν	-	0.276
b_{me}	-	-2.42 MPa
α'	-	$7.5 \cdot 10^{-4}$
α''	-	$3.5 \cdot 10^{-5}$

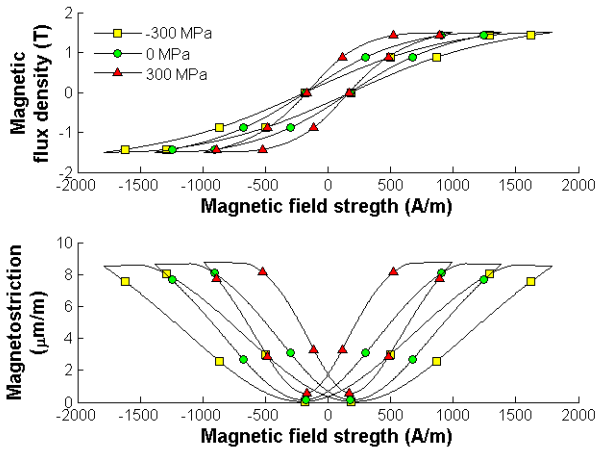

Fig. 1 Dependency of the hysteresis loops and magnetostriction on the field strength and the applied stress. Positive stress is tension.

B. Finite-Element Model and Implementation

A 1-D FE model for a ferromagnetic lamination is used for the simulations. A lamination with a thickness d and conductivity σ is considered. The unidirectional magnetodynamic field in the sheet is described by

$$\frac{\partial^2 h(z,t)}{\partial z^2} = \sigma\frac{\partial b(z,t)}{\partial t}. \tag{10}$$

The equation is solved using a magnetic vector potential $a(z,t)$, for which $b = \partial a(z,t)/\partial z$, and the magnetomechanical material model from the previous section is applied assuming the external stress τ to be constant in time and space:

$$\frac{\partial h\left(b\left(a(z,t)\right),\tau\right)}{\partial z} = \sigma\frac{\partial a(z,t)}{\partial t}. \tag{11}$$

Owing to symmetry, only one half of the lamination thickness $z \in [0, d/2]$ has to be modeled. To impose a certain average flux density $b_{\mathrm{av}}(t)$ through the sheet, the boundary conditions are $a(0,t) = 0$ at the center of the lamination, and $a(d/2,t) = b_{\mathrm{av}}(t) \cdot d/2$ at the surface.

Spatial discretization is performed using the Galerkin weighted residual method with nodal shape functions $N_i(z)$ $i = 1, \ldots, n$. The shape functions and the nodal values of the vector potential are arranged in column vectors $\boldsymbol{N}(z) = (N_1(z), \ldots, N_n(z))$ and $\boldsymbol{a} = (a_1, \ldots, a_n)$, respectively. For the time

discretization, the backward-Euler scheme with time step Δt is used. The discretized weak form of the equation becomes

$$\int_0^{d/2}\left[\frac{d\boldsymbol{N}(z)}{dz}h(\boldsymbol{a},\tau)+\frac{\sigma}{\Delta t}\left(\boldsymbol{N}(z)\boldsymbol{N}(z)^{\mathrm{T}}\right)\boldsymbol{a}\right]dz=\boldsymbol{f}\,, \quad (12)$$

in which the right-hand side $\boldsymbol{f}$ includes values from the previous time step.

The hysteretic nonlinearity is dealt with by solving the system with the fixed-point iteration. The field strength is expressed using a constant reluctivity ν_{FP}, and taking into account the error by a residual r_{FP}:

$$h(b,\tau)=\nu_{\mathrm{FP}}b+r_{\mathrm{FP}}(b,\tau)\,. \quad (13)$$

Substituting this into (12) gives

$$(\boldsymbol{S}_{\mathrm{FP}}+\boldsymbol{T})\boldsymbol{a}=\boldsymbol{f}-\boldsymbol{r}_{\mathrm{FP}}(\boldsymbol{a},\tau)\,, \quad (14)$$

where

$$\boldsymbol{S}_{\mathrm{FP}}=\int_0^{d/2}\nu_{\mathrm{FP}}\left(\frac{d\boldsymbol{N}(z)}{dz}\right)\left(\frac{d\boldsymbol{N}(z)}{dz}\right)^{\mathrm{T}}dz\,, \quad (15)$$

$$\boldsymbol{T}=\frac{\sigma}{\Delta t}\int_0^{d/2}\boldsymbol{N}(z)\boldsymbol{N}(z)^{\mathrm{T}}\,dz\,, \quad (16)$$

$$\boldsymbol{r}_{\mathrm{FP}}(\boldsymbol{a},\tau)=\int_0^{d/2}\frac{d\boldsymbol{N}(z)}{dz}r_{\mathrm{FP}}(\boldsymbol{a},\tau)\,dz\,. \quad (17)$$

Now the solution for $\boldsymbol{a}$ is iterated by starting from an initial value $\boldsymbol{a}^0$, and changing the value at iteration step i to

$$\boldsymbol{a}^i=(\boldsymbol{S}_{\mathrm{FP}}+\boldsymbol{T})^{-1}\left(\boldsymbol{f}-\boldsymbol{r}_{\mathrm{FP}}(\boldsymbol{a}^{i-1},\tau)\right). \quad (18)$$

As the initial value for each iteration round, the solution from the previous time step is used.

From the solution of the vector potential, the hysteresis and eddy-current losses, respectively, are averaged over one supply period discretized in n_{per} time steps as

$$p_{\mathrm{hy}}=\frac{1}{n_{\mathrm{per}}}\sum_{k=1}^{n_{\mathrm{per}}}\frac{2}{d}\int_0^{d/2}h(\boldsymbol{a}_k,\tau)\left(\frac{d\boldsymbol{N}(z)}{dz}\right)^{\mathrm{T}}\frac{\boldsymbol{a}_k-\boldsymbol{a}_{k-1}}{\Delta t}dz \quad (19)$$

$$p_{\mathrm{cl}}=\frac{1}{n_{\mathrm{per}}}\sum_{k=1}^{n_{\mathrm{per}}}\frac{2}{d}\int_0^{d/2}\sigma\left(\boldsymbol{N}(z)^{\mathrm{T}}\frac{\boldsymbol{a}_k-\boldsymbol{a}_{k-1}}{\Delta t}\right)^2dz\,. \quad (20)$$

III. Results and Discussion

A. Dynamic Magnetostriction

First, the effect of supply frequency on the surface magnetostriction is studied in a d = 0.5 mm, σ = 3 MS/m Fe-Si lamination. Fig. 2 shows the magnetostriction measured with an Epstein frame as a function of the average flux density at DC, 20 Hz and 50 Hz and 1.5 T. The FE model is applied at frequencies of 50, 100 and 200 Hz. After the FE solution of the skin-effect problem, the surface flux-density value is calculated and the surface magnetostriction is interpolated from the DC curve of Fig. 2. The simulated surface magnetostriction is plotted against the average flux density in Fig. 3. Although the exact shape is different from the measurements, the magnetostriction still shows dynamic hysteretic behavior with the enclosed area of the loop increasing with the frequency.

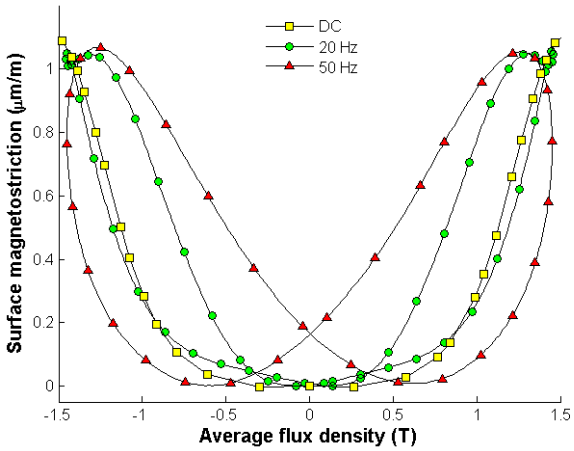

Fig. 2 Measured magnetostriction as a function of the average flux density at DC, 20 Hz and 50 Hz.

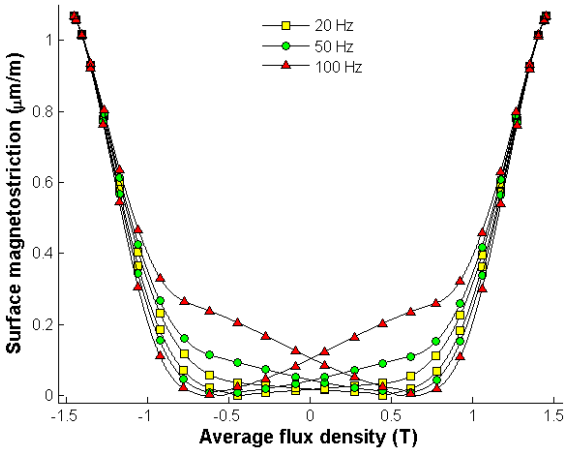

Fig. 3 Simulated "butterfly loops" i.e. surface magnetostriction vs. average magnetic flux density at different frequencies and zero applied stress.

The results imply that the dynamic behavior is at least partly caused by the skin effect of the eddy currents causing a phase lag between the average flux density and the local value of the magnetization on the surface, where the magnetostriction is calculated and also measured during experimental tests. Although the modeled surface magnetostriction rate-independent, the apparent dynamic effect is caused by comparison of a local quantity to a global one. This is analogous to dynamic hysteresis in magnetization loops, the origin of which is known to be explained by the skin effect [12]-[14].

The differences between the measurements and the simulations may be partly caused by the fact that the model does not account for the mechanical stiffness. In reality, the material cannot deform freely and thus the magnetostriction acts more like an equivalent body force which together with the stiffness defines the strain. In addition, any local rate-dependent behavior or excess eddy currents close to the surface are not accounted for in the model.

B. Dependency of Iron Losses on Stress

Secondly, the dependency of iron losses on the applied stress is studied in a 2 mm, 8 MS/m lamination. The FE model is solved for supply frequencies of 50-500 Hz and for average flux-density amplitudes of 0.6, 1.5 and 2.1 T. The results between 300-MPa compressive and 300-MPa tensile stresses are compared.

In Fig. 4 the difference between the losses obtained under the compressive and tensile stresses is shown relative to the compressive case. The hysteresis losses are higher under compressive stresses at low flux densities. However, after the material reaches saturation, the effect of the stress on the total area enclosed by the *b*-*h* loops is reduced, and thus the losses become only little affected.

The eddy-current losses are also affected by the effect of the stress on the material properties. At 100-Hz frequency, the losses at 0.6 T are 21.9 % higher in the compressive case than in the tensile case. At 1.5 and 2.1 T, the corresponding differences are -4.3 % and -7.5 %, respectively, which means that the losses are lower in the compressive case. These effects on the macroscopic eddy-current losses cannot be observed if only the statistical loss theory (1) is considered.

If the excess losses are calculated by subtracting the middle term of (1) from the numerically calculated eddy-current losses, the differences in the excess losses between the compressive and tensile cases at 100 Hz are +63 %, +215 %, and +81 % at 0.6, 1.5 and 2.1 T, respectively. These differences seem quite high and may lead to the conclusion that the excess losses are more seriously affected by the mechanical loading than the classical ones. At 0.6-T excitation the material remains fairly linear, and the uniformity assumption yields greater losses than the accurate skin-effect model. This causes the excess loss to be negative.

Although the domain structure was not considered in this paper, it is acknowledged that the macroscopic eddy-current losses alone probably cannot fully explain the increase in the iron losses, and that the excess eddy currents induced by domain-wall motion can still be significantly affected by the mechanical loading. The importance of the skin effect was here purposefully emphasized by studying a thick and highly-conducting lamination which are used, e.g., in synchronous machine rotors. It is likely that for thinner laminations, the effects are smaller. However, with the SJA model parameters used in this paper, the magnetization characteristics are quite little affected by the stresses when compared to the ones in [15]. A comprehensive identification with stress-dependent magnetization data should be performed to fully assess the effect in electrical steel sheets.

IV. Conclusion

An FE model was applied to study the coupling between magnetoelastic effects and eddy currents in ferromagnetic laminations. Accurate skin-effect modeling at least partly explains the apparent rate-dependency of magnetostriction. In addition, the mechanical loading was shown to affect also the macroscopic eddy-current losses, unlike predicted by the statistical loss theory. The presented findings should be considered for accurate analysis of vibrations and power losses in the cores of transformers and electrical machines.

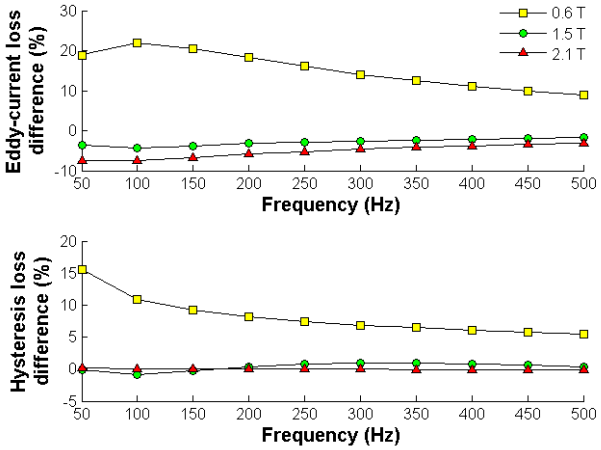

Fig. 4 Simulated relative difference in the eddy-current and hysteresis losses between the 300-MPa compressive and 300-MPa tensile cases.

References

[1] M. J. Sablik, D. C. Jiles, "Coupled Magnetoelastic Theory of Magnetic and Magnetostrictive Hysteresis," *IEEE Trans. Magn.*, Vol. 29, No. 3, pp. 2113-2123, July, 1993.

[2] D. C. Jiles, "Theory of the magnetomechanical effect," *J. Appl. Phys.*, Vol. 28, No. 8, pp. 1537-1546, August 1995.

[3] K. Fonteyn, A. Belahcen, R. Kouhia, P. Rasilo, A. Arkkio, "FEM for Directly Coupled Magneto-Mechanical, Phenomena in Electrical Machines," *IEEE Trans. Magn.*, Vol. 46, No. 8, pp. 2923-2926, August 2010.

[4] A. J. Moses, A. Ntatsis, T. Kochmann, J. Schneider, "Magnetostriction in non-oriented electrical steels: general trends," *J. Magn. Magn. Mater.*, Vol. 215-216, pp. 669-672, June 2000.

[5] T. Hilgert, L. Vandevelde, J. Melkebeek, "Neural-Network-Based Model for Dynamic Hysteresis in the Magnetostriction of Electrical Steel Under Sinusoidal Induction," *IEEE Trans. Magn.*, Vol. 43, No. 8, pp. 3462-3466, August 2007.

[6] K. Fonteyn, "Energy-Based Magneto-Mechanical Model for Electrical Steel Sheets," Ph.D. dissertation, Aalto University, 2010. Available at: http://lib.tkk.fi/Diss/2010/isbn9789526032887/.

[7] S. Somkun, A. J. Moses, P. I. Anderson, "Measurement and Modeling of 2-D Magnetostriction of Nonoriented Electrical Steel," *IEEE Trans. Magn.*, Vol. 48, No. 2, pp. 711-714, February 2012.

[8] V. Permiakov, L. Dupré, A. Pulnikov, J. Melkebeek, "Loss separation and parameters for hysteresis modelling under compressive and tensile stresses," *J. Magn. Magn. Mater.*, Vol. 272-276, pp. 553-554, January, 2004.

[9] D. Miyagi, N. Maeda, Y. Ozeki, K. Miki, N. Takahashi, "Estimation of Iron Loss in Motor Core With Shrink Fitting Using FEM Analysis," *IEEE Trans. Magn.,* Vol. 45, No. 3, pp. 1704-1707, March 2009.

[10] G. Bertotti, "General Properties of Power Losses in Soft Ferromagnetic Materials," *IEEE Trans. Magn.*, Vol. 24, No. 1, pp. 621-630, January 1988.

[11] I. Mayergoyz, "Nonlinear Diffusion of Electromagnetic Fields and Excess Eddy-Current Losses," *J. Appl. Phys.*, Vol. 85, No. 8, pp. 4910-4912, April 1999.

[12] R. M. Del Vecchio, "The Calculation of Eddy Current Losses Associated with Rotating Magnetic Fields in Thin Laminations", *IEEE Trans. Magn.*, Vol. 18, No. 6, pp. 1707-1709, November 1982.

[13] O. Bottauscio, M. Chiampi, D. Chiarabaglio, "Advanced Model of Laminated Magnetic Cores for Two-Dimensional Field Analysis", *IEEE Trans. Magn.*, Vol. 36, No. 3, pp. 561-573, May 2000.

[14] P. Rasilo, E. Dlala, K. Fonteyn, J. Pippuri, A. Belahcen, A. Arkkio, "Model of Laminated Ferromagnetic Cores for Loss Prediction in Electrical Machines," *IET Electr. Power Appl.*, Vol. 5, No. 7, pp. 580-588, August 2011.

[15] L. Bernard, X. Mininger, L. Daniel, G. Krebs, F. Bouillaut, M. Gabsi, "Effect of Stress on Switched Reluctance Motors: A Magneto-Elastic Finite-Element Approach Based on Multiscale Constitutive Laws," *IEEE Trans. Magn.*, Vol. 47, No. 9 pp. 2171-2178, September 2011.